Green Synthesis And Characterization Of Carboxymethyl Cellulose-Stabilized Silver Nanoparticles With Evaluation Of Antibacterial And Anticancer Activity

Oshin M Manchu[1*], Dr. S. Jasmin Sugantha Malar[2]

[1*]Research Scholar, Reg: No: 22213282032005, Department of Chemistry and Research Centre, Women's Christian College, Nagercoil - 629001. Affiliated to Manonmaniam Sundaranar University, Abishekapatti, Tirunelveli - 627012, Tamil Nadu, India. E-mail: oshinmanchu2000@gmail.com

[2]Associate Professor & Research Supervisor, Department of Chemistry and Research Centre, Women's Christian College, Nagercoil -629001. Affiliated to Manonmaniam Sundaranar University, Abishekapatti, Tirunelveli - 627012, Tamil Nadu, India. E-mail: lovelinjasmin@gmail.com

Abstract

Silver nanoparticles stabilized by carboxymethyl cellulose (CMC-AgNPs) were produced through an environmentally friendly approach and subsequently examined using UV-visible spectroscopy, X-ray diffraction (XRD), transmission electron microscopy (TEM), scanning electron microscopy (SEM), and energy dispersive X-ray spectroscopy (EDS). The UV-Visible spectrum revealed a surface plasmon resonance (SPR) peak at 426 nm, which confirms the successful synthesis of the nanoparticles. The crystalline nature of the synthesized nanoparticles was confirmed by XRD, and diffraction peaks were characteristic of the planes (111), (200), (220), (311), and (222) of face-centered cubic silver. The resultant crystallite sizes were in the range of 2.4–5.3 nm to support nanoscale dimensions. TEM analysis indicated well-dispersed ultrasmall nanoparticles with an average size of ~4 nm, which suggested the effective stabilization of CMC-induced nanoparticle formation and absence of agglomeration. SEM imaging depicted a quasi-spherical morphology with a consistent distribution throughout the CMC matrix. EDS spot analysis confirmed the presence of metallic silver, while area-scan spectra indicated the presence of carbon (C), oxygen (O), and trace elements linked to the polymer stabilizer. The biological effectiveness of CMC-AgNPs was evaluated against *Propionibacterium acnes* and MCF-7 breast cancer cells. In antibacterial assays, CMC-AgNPs showed no inhibitory effect on P. acnes at concentrations reaching 1000 nmol/well, whereas erythromycin (the positive control) consistently generated inhibition zones of 35 mm. In contrast, cytotoxicity assessments showed a concentration-dependent inhibition of MCF-7 cells, with an IC_{50} value of 61.20 µg/mL, along with morphological changes indicative of apoptosis or necrosis. These findings suggest that CMC-AgNPs were not effective against bacteria responsible for acne and they exhibited significant anticancer properties that highlighting the importance of nanoparticle surface chemistry in affecting biological activity.

Keywords: Carboxymethyl cellulose, Silver nanoparticles, Green synthesis, Anticancer activity, Acne bacteria, MCF-7 cells.

Introduction

Silver nanoparticles (AgNPs) have gained great scientific attention because of their remarkable physicochemical characteristics and broad biological properties, which in particular have been used in antimicrobial and anticancer applications [1]. Carboxymethyl cellulose is a widely used stabilizing agent due to its excellent biodegradability, hydrophilicity, non-toxicity and high metal-binding potential, which helps nanoparticle stabilization and prevents aggregation among other stabilizing agents [2] [3].

Acne vulgaris, mainly colonized by *Propionibacterium acnes*, is still a common skin inflammatory disorder. As with many medicines, it is not uncommon to use antibiotics such as erythromycin and clindamycin, but the growing problem of antimicrobial resistance has made new therapeutics essential. AgNPs can serve as effective alternative drugs by breaching bacterial membranes by ROS production, and compromising metabolism [4] [5].

Concurrently, breast cancer remains a significant global health problem and traditional chemotherapeutic modalities are plagued by systemic toxicity and resistance. Recent studies have shown that AgNPs have the ability to selectively promote apoptosis in cancer cells via ROS production, mitochondrial membrane disruption and DNA damage mechanisms [6]. Although CMC-stabilized AgNPs have been investigated on their own for biological applications, studies are still lacking to the ability of comparison their antibacterial and anticancer activities. The analysis of the effect of CMC surface chemistry on biological responses offers insight into how to design nanoparticles for specific applications. Consequently, the aims of this work were to:

(i) synthesize and characterize CMC-AgNPs by means of spectroscopic and microscopic methods,
(ii) evaluate their antibacterial activity against P. acnes,
(iii) evaluate their cytotoxic potential towards MCF-7 breast cancer cells by means of the MTT assay.

Materials and Methods

Synthesis of Carboxymethyl cellulose silver nanoparticles

For the green synthesis of CMC-AgNPs, CMC was purchased from SRL Chemicals, $AgNO_3$ from Molychem, and deionised water (ISO Chem Laboratories) was used throughout the study. Before being used, all glassware was thoroughly cleaned and rinsed with deionized water.

Carboxymethyl cellulose (650 mg) was dissolved in 150 ml deionized water. A solution of silver nitrate was prepared by dissolving 0.510 g $AgNO_3$ in 200 ml deionized water. 50 mL of the $AgNO_3$ solution was then taken and added to the CMC solution. The mixture was stirred and heated with a magnetic stirrer for 5 h. The formation of silver nanoparticles was indicated by the colour change from off-white colour to brown. The resulting silver nanoparticles were recovered, dried, and kept for further analysis.

The prepared CMC–AgNPs were characterized by using UV-Visible spectroscopy, Scanning Electron Microscopy (SEM), Energy-Dispersive X-ray Spectroscopy (EDS), TEM and XRD. The bioactivities such as anti-acne and anticancer activity were also tested.

Results and discussion

UV–visible Spectral Analysis

The optical absorption characteristics of the synthesized carboxymethyl cellulose-silver nanoparticles (CMC-AgNPs) were examined utilizing a Shimadzu UV-1800 double-beam spectrophotometer (Kyoto, Japan). The analysis of the samples took place in a 1.0 cm quartz cuvette, with deionized water acting as the baseline reference [7].

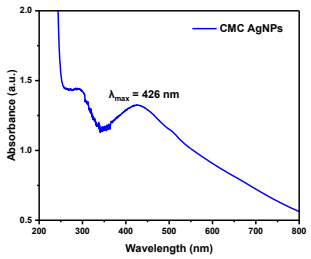

Figure 1. UV-visible spectrum of CMC-AgNPs with SPR peak at 426 nm

The UV–visible absorption spectrum of CMC-AgNPs (Figure 1) shows an obvious surface plasmon resonance (SPR) band at λ_{max} = 426 nm, which is the characteristic sign of metallic Ag^0 nanoparticles. The SPR band position is in the region of quasi-spherical silver nanoparticles stabilized in a polysaccharide medium. The sharpness and symmetry of the band, as well as the lack of secondary peaks or long-wavelength shoulders indicate a relatively narrow size distribution and low aggregation. A small shoulder at 250 nm is also noted which may be due to $\pi \rightarrow \pi^*$ transitions in the CMC backbone (carboxyl and polysaccharide moieties) or lingering Ag–ligand interactions, not an additional plasmonic resonance. This dual property including visible plasmon band as well as UV ligand transitions was extensively reported in polysaccharide-capped AgNPs, confirming the ability of reducing the silver ions to the metallic nanoparticles successfully and further stabilization [8].

X-ray Diffraction (XRD) Analysis

X-ray Diffraction (XRD) characterization of the CMC-AgNPs was conducted using a Bruker D8 Advance X-ray Diffractometer with a Cu Kα radiation source (λ = 1.5406 Å) in a 40 kV and 30 mA setting. Powdered samples were uniformly distributed on the sample holder, and diffraction patterns were recorded in a value range of 2θ 5°–90° with a step size of 0.02°. Peak positions and FWHMs were calculated from the peak-fitting software. Interplanar spacing was determined by Bragg's law and crystallite sizes were calculated by Scherrer equation assuming a shape factor of 0.90 [9].

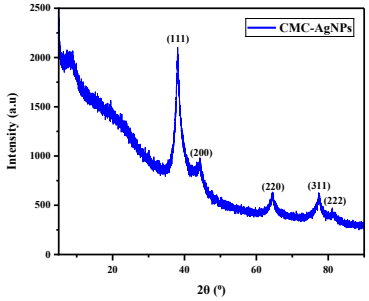

Figure 2. X-ray diffraction spectrum of CMC-AgNPs

Table 1. XRD peak data and calculated parameters of CMC-AgNPs

Peak	2θ (°)	FWHM β (°)	θ (°)	β (rad)	d (Å) (Bragg)	Crystallite size D (nm)	Microstrain ε ($\times 10^{-2}$)
(111)	38.0097	1.5798	19.0049	0.027579	2.36544	**5.32**	2.00
(200)	44.3206	3.5436	22.1603	0.061855	2.04216	**2.42**	3.80
(220)	64.2604	2.1848	32.1302	0.038148	1.44835	**4.29**	1.52
(311)	77.5144	1.9654	38.7572	0.034295	1.23047	**5.18**	1.07
(222)	81.7552	3.3197	40.8776	0.057934	1.17703	**3.17**	1.67
Average						**4.08**	

XRD of carboxymethyl cellulose silver nanoparticles (CMC-AgNPs) reveals the presence of five different diffraction peaks with a 2θ of 38.01°, 44.32°, 64.26°, 77.51° and 81.76°. These peaks are related to the planes of (111), (200), (220), (311) and (222) of the face-centered cubic (fcc) silver, thus verifying crystalline metallic Ag^0's formation. The calculated d-spacing in accordance with Bragg's law well reflected the normal JCPDS file (04-0783) when compared to silver that further verified the successful reduction of Ag^+ to Ag^0 form. The highest intensity (38°,111) of the diffraction peak suggests that the nanoparticles have slight tendency of (111) preference which is typical in chemically and polymer stable AgNPs. The peak widths were computed by the Scherrer equation, and crystallite size was 2.42–5.32 nm with an average of ~4.08 nm. Due to the small crystals, CMC may effectively suppress nanoscale nucleation leading to an uncontrollable growth pattern by acting as a stabilizing and capping agent. All reflections contained slight peak broadening consistent with nanoscale domains and light lattice strain. The calculated microstrain numbers (0.010–0.038) have confirmed that the strain is small, where the particles were well-stabilized and produced little structural distortion. No Impurity peaks attributed to silver oxide or byproducts were observed in Figure 2, confirming the high purity of synthesized nanoparticles [10].

SEM-EDS Analysis

The morphology of the nanoparticles was analyzed utilizing a FEI Quanta FEG 200F scanning electron microscope which was operated at an accelerating voltage of 15 kV and a working distance of 10 mm. Elemental composition was analyzed by means of an Oxford Instruments INCA energy dispersive X-ray spectroscopy (EDS) system attached to the SEM. Spectra were measured at 20 kV accelerating voltage with a live time of 60 s and a take-off angle of 35°. In addition, quantification was made by means of ZAF correction (atomic number, absorption, fluorescence). Spot-scan spectra (localized bright regions) and area-scan spectra (nanoparticles + polymer matrix) were captured for complementing this analysis of the composite [11] [12].

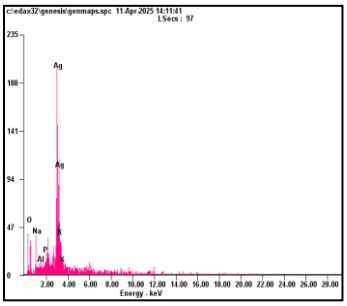

Figure 3. SEM of CMC-AgNPs

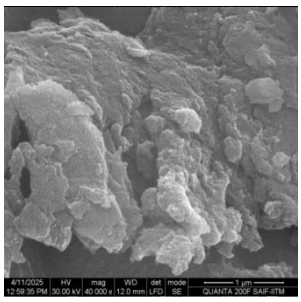

Figure 4. EDS spectrum of CMC-AgNPs

Table 2. Elemental composition (Wt% & At%) of CMC-AgNPs

Element	***Wt%***	***At%***
O	31.75	63.45
Na	10.48	14.58
Al	02.37	02.80
P	02.73	02.82
Ag	51.26	15.19

SEM micrograph (Figure 3) shows bright, nearly spherical nanoparticles across the dark organic background of CMC, confirming that AgNPs are embedded in the polymer matrix. To determine the elemental composition, the EDS spectrum (Figure 4) (Table 2) revealed the presence of O (31.75 wt%, 63.45 at%), Na (10.48 wt%, 14.58 at%), Al (2.37 wt%, 2.80 at%), P (2.73 wt%, 2.82 at%), Ag (51.26 wt%, 15.19 at%) and K (1.40 wt%, 1.15 at%) [13] [14]. High Ag content demonstrates the formation of silver nanoparticles, while oxygen and sodium come from the CMC stabilizing matrix. Besides Ag, minor peaks of Na, Al, P and K are likely derived from the CMC stabilizing matrix and residual ionic species from the synthesis process, implying that they are surface-associated rather than metallic nanoparticle components [15].

Transmission Electron Microscopy (TEM)

The transmission electron microscopy (TEM) analysis of carboxymethyl cellulose silver nanoparticles (CMC-AgNPs) was also carried out with a FEI Tecnai G2 F30 S-TWIN Transmission Electron Microscope operated at 300 kV. Upon application to the nanoparticle, a uniform suspension was obtained by dispersion in ethanol after sonication. A drop of the well dispersed sample was transferred to a carbon-coated copper grid to dry at room temperature.

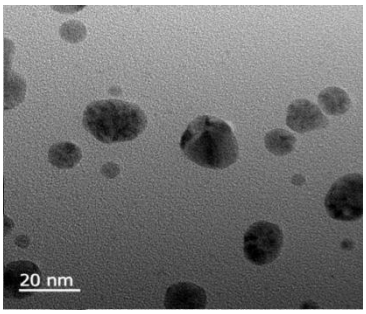

Figure 5. TEM micrograph showing CMC-AgNPs

The TEM analysis of the carboxymethyl cellulose silver nanoparticles (CMC-AgNPs) revealed that the particles are round in shape and well dispersed. The size of the particles from the TEM image was approximately 4.362 nm, representing ultrasmall nanoparticles. The nanoscale nature of those features is clearly indicated in the scale bar of the micrograph (20 nm). The standardized size and circular pattern could indicate CMC was a good stabilizing and capping agent in fact, which also prevented particle growth and aggregation. It can also be verified that the particle boundaries and smooth outlines were clearly observed on the TEM image, indicating that the nanoparticles are well-distributed and discrete [16]. A similar size to ~4 nm matches the crystallite size obtained by XRD, which indicates that synthesized CMC–AgNPs are very uniform and crystalline at the nanometer level. TEM showed that the prepared carboxymethyl cellulose silver nanoparticles were round shaped and good dispersion material with a mean particle size of approximately 4 nm. That the CMC stabilized the small sized AgNPs uniformly, thus successful formation of ultrasmall AgNPs which are readily dispersed, is clear [17].

Antibacterial activity

Antibacterial activity of CMC-AgNPs against *P. acnes* (MTCC 1951) was tested at the Microbial Type Culture Collection and Gene Bank (MTCC), Chandigarh, India. Mueller-Hinton Agar (MHA; SRL-Chem, Cat. No. 24756) plates were utilized for the growth medium. The bacterial inoculum was grown in Mueller-Hinton Broth and was standardized at 0.5 McFarland turbidity corresponding to ~1.5×10^8 CFU/mL cell density. For the assay, 100 µL of the standardized culture was spread uniformly on MHA plates. In the agar, wells were built via a sterile borer. A volume of thirty µL of the test substance was introduced into each well. CMC-AgNPs were prepared as a 10% stock solution, followed by serial dilutions to achieve final test concentrations ranging from 62.5-1000 nmol/well. As vehicle control, DMSO was used to confirm that the solvent had no antimicrobial effect. Erythromycin (5 µg, SRL-Chem, Cat. No. 78079) was employed as the positive control to confirm the reliability of the assay. The plates were incubated 24 hours at 37 °C for the inoculated plates. After incubation, the antibacterial activity was measured by measuring the diameter of a clear zone of inhibition near each well. Values were recorded in millimeters, and averages were calculated between triplicate plates [18] [19].

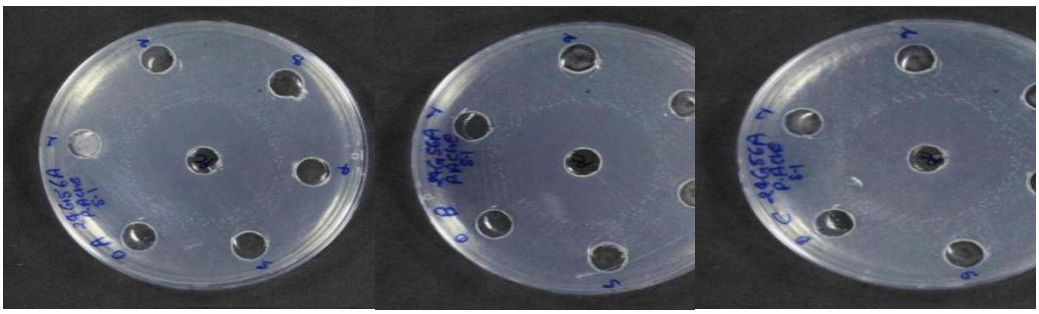

Figure 6a, 6b, 6c. Triplicate antibacterial well diffusion plates of CMC-AgNPs

Table 3. Zone of inhibition values (mm) for CMC-AgNPs

Amount (nmol/well)	**Plate A**	**Plate B**	**Plate C**	**Average**	Standard Deviation	Standard Error of Mean
PC	35	35	35	35	0	0

0	0	0	0	0	0	0
62.5	0	0	0	0	0	0
125	0	0	0	0	0	0
250	0	0	0	0	0	0
500	0	0	0	0	0	0
1000	0	0	0	0	0	0

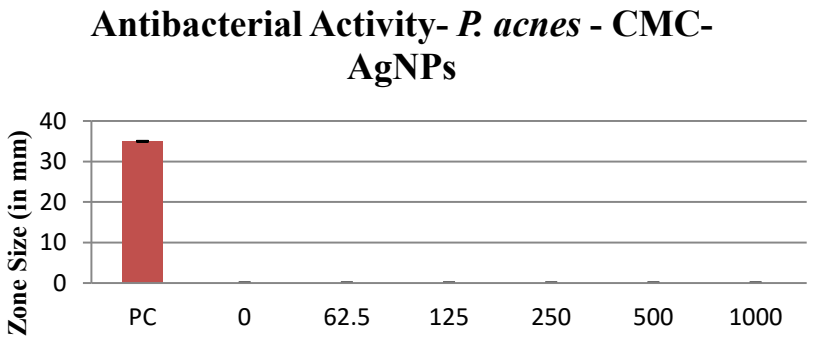

Figure 7. Antibacterial activity of CMC-AgNPS against *P.acnes*

Table 4. Zones of inhibition results for CMC-AgNPs compared with positive control

S. No.	Sample Id	Concentration	Average Zone of inhibition (mm)
1	Erythromycin (PC)	5µg	35
2	CMC-AgNPs	-	-

Table 4 summarizes the antibacterial activity of CMC-AgNPs against *P. acne*s. AgNP concentrations are expressed in nmol/well while erythromycin is expressed in µg. The positive control erythromycin showed a clear zone of drug inhibition of 35 mm across the replicates, under all tests and all analyses confirmed the reliability for the assay. The vehicle (DMSO) control exhibited no inhibition, confirming that the solvent without the other compounds did not affect bacterial growth. CMC-AgNPs at 62.5, 125, 250, 500, and 1000 nmol/well were not associated with any measurable inhibition zones. There is no activity to observe in every replicate compared to the tested two types of nanoparticles indicating that the nanoparticles had no antibacterial function under the tested conditions. The results clearly show that CMC-AgNPs did not show antibacterial activity against *P. acnes* up to 1000 nmol/well. Here, we expect various factors to explain this result. It was suggested that the CMC coating on the nanoparticles would have inhibited the release of Ag^+ ions (a key source of antimicrobial activity) for several reasons. *P. acnes* is able to form biofilms, and biofilm formation markedly lowers the susceptibility of bacteria to antimicrobial agents. Biofilm features protective extracellular polymeric components that provide a barrier against nanoparticle penetration. In the same way, it has been observed in other studies that silver nanoparticles can have antibacterial activity primarily by interfering in the cell membrane, producing oxidative stress and disrupting DNA synthesis activity [20]. Nevertheless these effects are closely dependent on properties of nanoparticles: size, shape, surface charge and coating. In our case the stabilizing function of CMC may have made it difficult for AgNPs to interact with bacterial cells, thereby neutralizing their antimicrobial potential. This indicates that surface capping by CMC significantly limits Ag^+ ion release, which is essential for antibacterial activity. The vigorous antibacterial activity of erythromycin in this study demonstrated the validity of the assay and brought the challenge of reproducing the efficacy of conventional antibiotics using polymer-coated nanoparticles [21].

Anticancer activity

MCF-7 cells (human breast adenocarcinoma; NCCS, Pune) were grown on Dulbecco's Modified Eagle Medium (DMEM, high glucose; Gibco) containing 10% fetal bovine serum (HiMedia) and 1% antibiotic–antimycotic. Cells were cultured at 37 °C in a humidified incubator with 5% CO_2 and 18–20% O_2 and subcultured every 48 h; cells at passage number 75 were used for cytotoxicity studies. Twenty thousand cells were seeded per well in a 96-well culture plate with 200 µL of medium and allowed to adhere overnight for this assay. They were then exposed to CMC-AgNPs at 6.25, 12.5 and 25, 50 and 100 µg/mL for 24 h: untreated cells were the negative control and doxorubicin (1 µg/mL) the positive control. Following treatment, MTT reagent (0.5 mg/mL final concentration) was added to the medium and the plates were incubated for 3 h in the dark. After incubation, the MTT reagent was discarded and a dissolution of formazan crystals in 100 µL of dimethyl sulfoxide (DMSO). Absorbance values were measured at 570 nm by a microplate reader (BioTek ELX-800). The results are shown in table 5 and 6. Cell viability (%) was computed. % Cell viability is calculated using below formula:

$$\% \text{ cell viability} = \frac{\text{Absorbance of treated cells}}{\text{Absorbance of untreated control cells}} \text{x } 100$$

The IC_{50} value was determined by using linear regression equation i.e. y=mx+c

Table 5. MTT assay showing absorbance, cell viability (%) and IC_{50}values of CMC-AgNPs

Concentration Unit: µg/mL		**Incubation:24hrs**			**Cell line: MCF7**			**PN-75**
Parameter	**Blank**	**Untreated**	**Dox-1µg**	**6.25**	**12.5**	**25**	**50**	**100**
Abs reading 1	0.086	2.533	1.343	2.209	2.068	1.874	1.318	0.851
Abs reading 2	0.084	2.596	1.447	2.227	2.056	1.752	1.422	0.782
Mean abs	0.085	2.5645	1.395	2.218	2.062	1.813	1.37	0.8165
Mean abs (Sample-Blank)		2.4795	1.31	2.133	1.977	1.728	1.285	0.7315
STANDARD DEVIATION		0.044547727	0.073539105	0.012727922	0.008485281	0.086267027	0.073539105	0.048790368
STANDARD ERROR		0.0315	0.052	0.009	0.006	0.061	0.052	0.0345
Cell Viability %		**100**	**52.83323251**	**86.02540835**	**79.7338173**	**69.69147005**	**51.82496471**	**29.50191571**
IC_{50} value=61.20µg/mL								

Table 6. Dose dependent cell viability of MCF-7 cells treated with CMC-AgNPs and corrosponding IC_{50} value

MTT assay CMC-AgNPs vs MCF7 (% cell viability)	
Culture condition	**% cell viability**
Untreated	100.00
Dox-1µg	52.83
CMC-6.25µg	86.03
CMC-12.5µg	79.73
CMC-25µg	69.69
CMC-50µg	51.82
CMC-100µg	29.50
IC_{50} conc (µg/mL)	**61.20µg/mL**

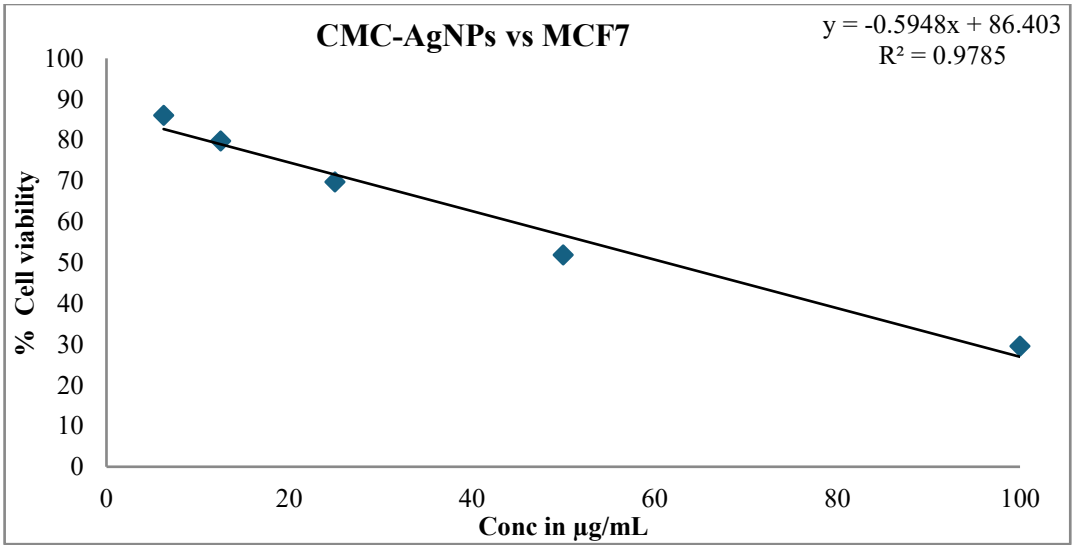

Figure 8. Dose-response curve showing the reduction in MCF-7 cell viability with increasing concentrations of CMC-AgNPs.

CMC-AgNPs clearly demonstrate concentration-dependent cytotoxicity towards MCF-7 breast cancer cells. Decreased cell viability from 86.03% at 6.25 µg/mL to 29.50% at 100 µg/mL indicates a high potential inhibitory effect. The IC_{50} of 61.20 µg/mL obtained indicates that the compounds have moderate cytotoxic efficiency, comparable to existing chemotherapeutics in in vitro models. The morphological modification seen microscopically also validates the quantitative MTT assay, as cells grown with high CMC-AgNPs concentration showed evidence that they show apoptosis or necrosis including shrinkage and loss of cell adherence. The experimental design was validated with the positive control (doxorubicin) yielding an approximate 53% viability at 1 µg/mL [22]. Under microscopic observation, marked morphological changes of MCF-7 breast cancer cells were detected after CMC-AgNPs treatment. These cells exhibited healthy appearance, were well-spread and adhered to surface with normal cellular shape. However, with higher concentrations of the nanoparticles, a decreasing number of cells and adherence in response to dose was found. At 25–50 µg/mL, cells also displayed a round shape with shrinkage and disruption of the tight junctions due to early cytotoxic response. At 100µg/mL drastic morphological damage, drop of cell integrity and considerable cell death were proved. These visible changes correlate with the MTT data determining that CMC - AgNPs contain effective anti proliferative activity against MCF - 7 cells [23] [24].

Commonly, the known cytotoxicity of AgNPs is attributed to their generation of reactive oxygen species (ROS), activation of oxidative stress pathway, and damage to cellular components including mitochondria and DNA. CMC stabilization prevents aggregation and improves bioavailability of nanoparticles that in turn increases their cellular uptake and cytotoxicity. Similar results were reported in other studies confirming that CMC-AgNPs showed significant anticancer activity against breast cancer cell lines [25] [26].

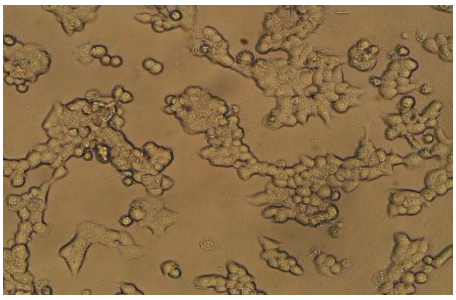

Figure 9a. Control – Healthy cells with normal morphology and full confluency.

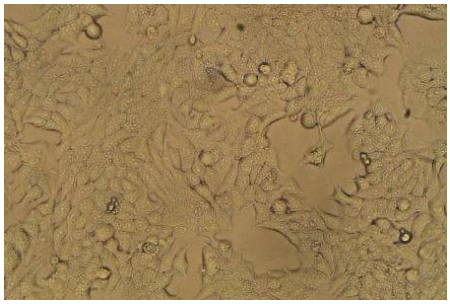

Figure 9b. Untreated – Cells appear intact, well-spread and adherent to the surface.

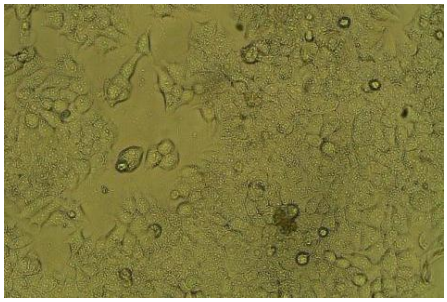

Figure 9c. 6.25 µg/mL – Slight reduction in cell density, early minor morphological changes.

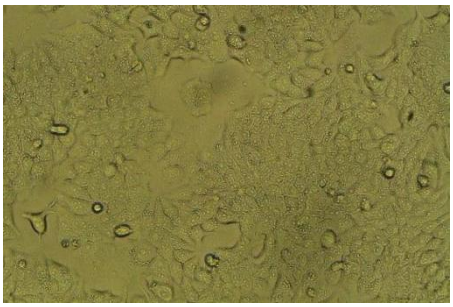

Figure 9d. 12.5 µg/mL – Noticeable rounding and decrease in viable cells.

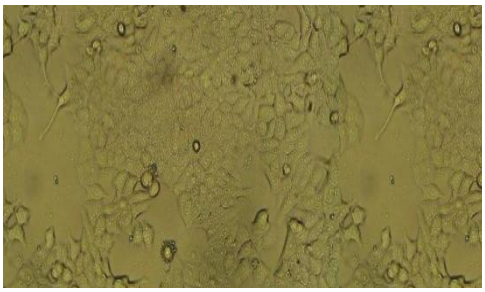

Figure 9e. 25 µg/mL – Cells show shrinkage and partial detachment.

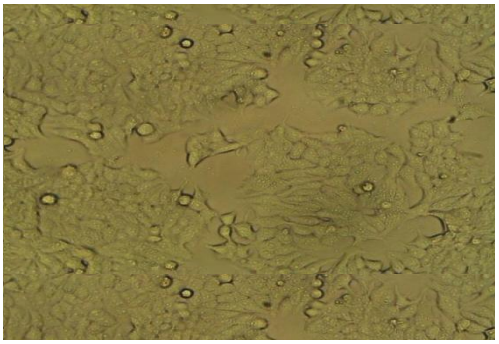

Figure 9f. 50 µg/mL – Marked cytotoxicity with loss of membrane integrity.

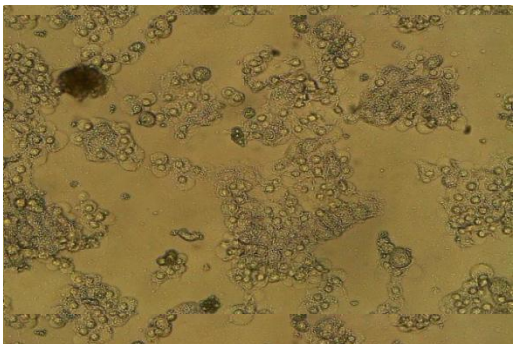

Figure 9g. 100 µg/mL – serious damage with broad cell death and disintegration.

Conclusion

Carboxymethyl cellulose-stabilized silver nanomaterials have been prepared in this study using the green technique and characterized using UV-visible spectroscopy, XRD, SEM-EDS and TEM. When synthesized, the CMC-AgNPs are completely controlled, durable and stable. The nanoparticles are noted for a sharp SPR peak at 426 nm, ultrasmall spherical morphology (~4 nm) and crystalline FCC structure exhibiting favorable stability. Antibacterial studies demonstrated no inhibition to *P. acnes* at 1000 nmol/well although this was based on a limitation of Ag^{+} ion release due to extreme CMC capping or biofilm formation resistance. In comparison, the nanoparticles exhibited significant cytotoxicity to MCF-7 breast cancer cells, with IC_{50} of 61.20 µg/mL and morphology reflecting cell death. In summary, CMC-AgNPs were ineffective anti-acne agents on the evaluated basis, but showed potential anticancer ability indicating that CMC-AgNPs might be of interest for cancer therapeutics, drug delivery, biomaterial coatings, or nanoparticles. Future studies consist of polymer concentration tuning towards ion release at higher concentration, surface charging changes, addition of plant

extracts or therapeutic compounds, nanocomposites fabrication to improve antibacterial capacity and to reach on a much broader range of bio-medicine applications.

Author contributions

Oshin M Manchu carried out the experiments, collected and analyzed the data, and wrote the original draft of the manuscript.

Dr. S. Jasmin Sugantha Malar supervised the research work and provided overall guidance.

Funding

The authors did not receive any financial support from any organization for this work.

Acknowledgement
The authors sincerely thank Manonmaniam Sundaranar University, Abishekapatti, Tirunelveli - 627012, Tamil Nadu for academic support. The authors also thank the Women's Christian College, Nagercoil-629001, for providing the necessary laboratory facilities to carry out this research work.

REFERENCES

1. Rai, M., Yadav, A. and Gade, A., 2009. Silver nanoparticles as a new generation of antimicrobials. *Biotechnology Advances*, 27(1), pp.76-83.
2. Shaaban, M.T., Mohamed, B.S., Zayed, M. and El-Sabbagh, S.M., 2024. Antibacterial, antibiofilm, and anticancer activity of silver-nanoparticles synthesized from the cell-filtrate of Streptomyces enissocaesilis. *BMC biotechnology*, 24(1), p.8.
3. Salem, S.S., Hashem, A.H., Sallam, A.A.M., Doghish, A.S., Al-Askar, A.A., Arishi, A.A. and Shehabeldine, A.M., 2022. Synthesis of silver nanocomposite based on carboxymethyl cellulose: Antibacterial, antifungal and anticancer activities. *Polymers*, 14(16), p.3352.
4. Platsidaki, E. and Dessinioti, C., 2018. Recent advances in understanding Propionibacterium acnes (Cutibacterium acnes) in acne. *F1000Research*, 7, pp.F1000-Faculty.
5. Walsh, T.R., Efthimiou, J. and Dréno, B., 2016. Systematic review of antibiotic resistance in acne: an increasing topical and oral threat. *The Lancet Infectious Diseases*, 16(3), pp.e23-e33.
6. Khorrami, S., Zarrabi, A., Khaleghi, M., Danaei, M. and Mozafari, M.R., 2018. Selective cytotoxicity of green synthesized silver nanoparticles against the MCF-7 tumor cell line and their enhanced antioxidant and antimicrobial properties. *International journal of Nanomedicine*, pp.8013-8024.
7. Kelly, K.L., Coronado, E., Zhao, L.L. and Schatz, G.C., 2003. The optical properties of metal nanoparticles: the influence of size, shape, and dielectric environment. *The Journal of Physical Chemistry B*, 107(3), pp.668-677.
8. Šileikaitė, A., Prosyčevas, I., Puišo, J., Juraitis, A. and Guobienė, A., 2006. Analysis of silver nanoparticles produced by chemical reduction of silver salt solution. *Materials science*, 12(4), pp.287-291.
9. Nasiri, S., Rabiei, M., Palevicius, A., Janusas, G., Vilkauskas, A., Nutalapati, V. and Monshi, A., 2023. Modified Scherrer equation to calculate crystal size by XRD with high accuracy, examples Fe2O3, TiO2 and V2O5. *Nano Trends*, 3, p.100015.
10. Bykkam, S., Ahmadipour, M., Narisngam, S., Kalagadda, V.R. and Chidurala, S.C., 2015. Extensive studies on X-ray diffraction of green synthesized silver nanoparticles. Adv. *Nanopart*, 4(1), pp.1-10.
11. Shi, D., Wang, F., Lan, T., Zhang, Y. and Shao, Z., 2016. Convenient fabrication of carboxymethyl cellulose electrospun nanofibers functionalized with silver nanoparticles. *Cellulose*, 23(3), pp.1899-1909.
12. Devi, L.S. and Joshi, S.R., 2015. Ultrastructures of silver nanoparticles biosynthesized using endophytic fungi. *Journal of Microscopy and Ultrastructure*, 3(1), pp.29-37.
13. Forough, M. and Farhadi, K., 2010. Biological and green synthesis of silver nanoparticles. *Turkish J. Eng. Env. Sci*, 34(4), pp.281-287.
14. Juan, L., Zhimin, Z., Anchun, M., Lei, L. and Jingchao, Z., 2010. Deposition of silver nanoparticles on titanium surface for antibacterial effect. *International journal of nanomedicine*, pp.261-267.
15. El-Shishtawy, R.M., Asiri, A.M., Abdelwahed, N.A. and Al-Otaibi, M.M., 2011. In situ production of silver nanoparticle on cotton fabric and its antimicrobial evaluation. *Cellulose*, 18(1), pp.75-82.
16. Hebeish, A.A., El-Rafie, M.H., Abdel-Mohdy, F.A., Abdel-Halim, E.S. and Emam, H.E., 2010. Carboxymethyl cellulose for green synthesis and stabilization of silver nanoparticles. *Carbohydrate polymers*, 82(3), pp.933-941.
17. Yunusov, K.E., Sarymsakov, A.A. and Rashidova, S.S., 2014. Structure and properties of biodegradable carboxymethyl cellulose films containing silver nanoparticles. *Polymer Science Series A*, 56(3), pp.283-288.
18. Dessinioti, C. and Katsambas, A., 2017. Propionibacterium acnes and antimicrobial resistance in acne. *Clinics in dermatology*, 35(2), pp.163-167.

19. Tang, S. and Zheng, J., 2018. Antibacterial activity of silver nanoparticles: structural effects. *Advanced healthcare materials*, 7(13), p.1701503.
20. Ruchiatan, K., Rizqandaru, T., Satjamanggala, P.R., Tache, N., Cahyadi, A.I., Rezano, A., Gunawan, H., Sutedja, E.K., Dwiyana, R.F., Hidayah, R.M.N. and Achdiat, P.A., 2023. Characteristics of biofilm-forming ability and antibiotic resistance of Cutibacterium acnes and Staphylococcus epidermidis from acne vulgaris patients. *Clinica*l, Cosmetic and Investigational Dermatology, pp.2457-2465.
21. Khalifa, H.O., Oreiby, A., Mohammed, T., Abdelhamid, M.A., Sholkamy, E.N., Hashem, H. and Fereig, R.M., 2025. Silver nanoparticles as next-generation antimicrobial agents: mechanisms, challenges, and innovations against multidrug-resistant bacteria. *Frontiers in cellular and infection microbiology*, 15, p.1599113.
22. Capanema, N.S., Carvalho, I.C., Mansur, A.A., Carvalho, S.M., Lage, A.P. and Mansur, H.S., 2019. Hybrid hydrogel composed of carboxymethylcellulose–silver nanoparticles–doxorubicin for anticancer and antibacterial therapies against melanoma skin cancer cells. *ACS Applied Nano Materials*, 2(11), pp.7393-7408.
23. Basta, A.H., El-Saied, H., Hasanin, M.S. and El-Deftar, M.M., 2018. Green carboxymethyl cellulose-silver complex versus cellulose origins in biological activity applications. *International journal of biological macromolecules*, 107, pp.1364-1372.
24. Al-Asiri, W.Y., Al-Sheddi, E.S., Farshori, N.N., Al-Oqail, M.M., Al-Massarani, S.M., Malik, T., Ahmad, J., Al-Khedhairy, A.A. and Siddiqui, M.A., 2024. Cytotoxic and Apoptotic Effects of Green Synthesized Silver Nanoparticles via Reactive Oxygen Species–Mediated Mitochondrial Pathway in Human Breast Cancer Cells. *Cell Biochemistry and Function*, 42(7), p.e4113.
25. Vizhi, D.K., Supraja, N., Devipriya, A., Tollamadugu, N.V.K.V.P. and Babujanarthanam, R., 2016. Evaluation of antibacterial activity and cytotoxic effects of green AgNPs against Breast Cancer Cells (MCF 7). *Advances in nano research*, 4(2), p.129.
26. Mosmann, T., 1983. Rapid colorimetric assay for cellular growth and survival: application to proliferation and cytotoxicity assays. *Journal of immunological methods*, 65(1-2), pp.55-63.